

# Polarization-Independent Light Emission Enhancement of ZnO/Ag Nanograting via Surface Plasmon Polariton Excitation and Cavity Resonance

Minji Gwon,<sup>†</sup> Y. U. Lee,<sup>†</sup> J. W. Wu,<sup>†</sup> Dahyun Nam,<sup>‡</sup> Hyeonsik Cheong,<sup>‡</sup> and Dong-Wook Kim<sup>\*,†</sup>

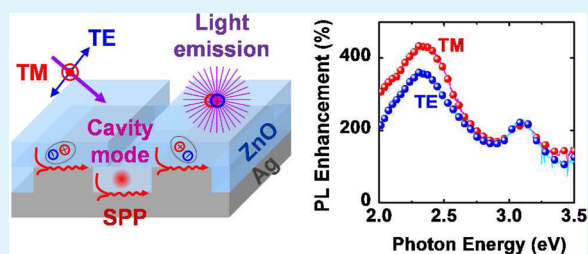
<sup>†</sup>Department of Physics and Quantum Metamaterials Research Center, Ewha Womans University, Seoul 120-750, Korea

<sup>‡</sup>Department of Physics, Sogang University, Seoul 121-742, Korea

## S Supporting Information

**ABSTRACT:** In this study, we observed that the photoluminescence (PL) intensity of ZnO/Ag nanogratings was significantly enhanced compared with that of a planar counterpart under illumination of both transverse magnetic (TM) and transverse electric (TE)-mode light. In the TM mode, angle-resolved reflectance spectra exhibited dispersive dips, indicating cavity resonance as well as grating-coupled surface plasmon polariton (SPP) excitation. In the TE mode, cavity resonance only was allowed, and broad dips appeared in the reflectance spectra. Strong optical field confinement in the ZnO layers, with the help of SPP and cavity modes, facilitated polarization-insensitive PL enhancement. Optical simulation results were in good agreement with the experimental results, supporting the suggested scenario.

**KEYWORDS:** nanograting, ZnO, surface plasmon polariton, cavity resonance



## INTRODUCTION

A grating is an optical component commonly used to manipulate light propagation based on diffraction phenomena. Additionally, metallic gratings can exhibit anomalous reflection spectra, due to excitation of surface plasmon polariton (SPP).<sup>1–9</sup> SPPs originate from the oscillatory motion of free carriers in metals, and generate propagating electromagnetic fields concentrated at the metal–dielectric interface. SPPs have a larger momentum than photons with identical energy; hence, coupling with the radiative electromagnetic field is possible with the help of the reciprocal lattice vector from periodic structures (i.e., gratings).<sup>1–19</sup> SPPs are associated with fascinating physical phenomena, including extraordinary optical transmission<sup>8,9</sup> and enhanced light absorption/emission.<sup>10–19</sup> Thus, extensive research has been devoted to understanding the nature of SPPs and the fabrication of novel periodic nanostructures for exploiting the beneficial roles of SPPs.

Semiconductor–metal grating structures exhibit interesting optical properties: tunable spectral response and high responsivity,<sup>10</sup> improved light emission,<sup>11–17</sup> and broadband enhanced optical reflectance.<sup>18,19</sup> ZnO is a key material in various applications due to its wide band gap energy, large refractive index, and material compatibility. Thus, the application of ZnO includes photodetectors,<sup>10</sup> fluorescent biosensors,<sup>14,15</sup> light-emitting diodes,<sup>16,17</sup> and back reflectors for thin-film solar cells.<sup>18,19</sup> In all these studies, the plasmonic effects in the ZnO/metal structures play major roles in improvement of the device performance. The SPP effects enable strong confinement of optical field at sub-wavelength

regime but they are allowed only with a wave vector oriented parallel to the grating vector of a one-dimensional (1D) grating.<sup>14</sup> Such polarization dependence would limit the performance of the grating-based optoelectronic devices. Additional mechanism, enabling less polarization dependence, would be desirable for further improvement of the device performance and the tunability of the spectral response.

In this study, we fabricated ZnO/Ag nanogratings and investigated their optical characteristics, in particular, their dependence on the incident light polarization. Angle-resolved optical reflectance spectra of the grating exhibited clear dispersive dips only when the electric field of the incident light was parallel to the grating groove, i.e., transverse magnetic (TM) mode. For transverse electric (TE)-mode light polarization, the reflection spectra displayed broad dips with little angle dependence. The photoluminescence (PL) spectra of the grating were much enhanced compared with those of its planar counterpart, under both TM and TE modes. Optical simulations of the gratings suggest that not only SPP effects, but also cavity resonance, contributed to the optical field distribution in the grating and enabled polarization-insensitive PL enhancement.

Received: March 11, 2014

Accepted: May 21, 2014

Published: May 21, 2014

## EXPERIMENTAL SECTION

1D Si nanograting structures (period: 500 nm; depth: 70 nm; area:  $100 \times 100 \mu\text{m}^2$ ) were fabricated by electron-beam lithography (JBX6000FS/E, JEOL) and dry etching (ICP 380, Oxford System) (see Supporting Information Figure S1). ZnO (120 nm)/Ag (80 nm) thin films were deposited on the Si nanograting by RF sputtering, as schematically illustrated in Figure 1. Detailed thin film deposition

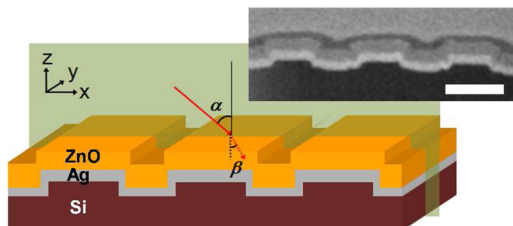


**Figure 1.** Schematic diagram and a cross-sectional scanning electron microscopy (SEM) image of the ZnO/Ag nanograting structure. The scale bar in the SEM image is 300 nm. The red arrow and shaded plane indicate the incident light and incident plane, respectively.  $\alpha$  and  $\beta$  correspond to the angles of incident light and refracted light at the air/ZnO surface, respectively.

conditions can be found in our earlier publication.<sup>11</sup> An angle-resolved micro-spectrophotometer was used to obtain the polarization-dependent reflection spectra of the grating sample. The tungsten-halogen lamp input light source produced a  $\sim 50\text{-}\mu\text{m}$ -diameter beam spot size on the sample surface. The angle of incidence ( $\alpha$  in Figure 1) was varied from  $15\text{--}60^\circ$ . The incident light was linearly polarized: the electric field was parallel to either the  $x$ -axis (TM mode) or the  $y$ -axis (TE mode). The reflected light was collected by a microscope objective and directed to a UV/VIS spectrometer (spectral range:  $400\text{--}1100\text{ nm}$ ) via an optical fiber. For micro-PL measurements, the sample was excited by a He–Cd laser (wavelength: 325 nm). The 1 mW laser beam was focused to a spot size  $\sim 2\text{ }\mu\text{m}$  in diameter, using a  $40\times$  microscope objective (0.5 NA). The signal was dispersed with a spectrometer (Jobin–Yvon TRIAX 320), and luminescence spectra were obtained by a thermoelectrically cooled back-illuminated charge-coupled device (CCD).

## RESULTS AND DISCUSSION

Figure 2a and b shows the angle-resolved reflectance ( $R$ ) spectra of the ZnO/Ag nanograting as a function of photon energy and incident angle ( $\alpha$ ). The TM-mode reflectance spectra have several reflectance dips showing clear incident angle dependence. The overall reflectance of the TE mode was smaller than that of the TM mode and had broad minima at  $\sim 2\text{ eV}$  and  $\alpha \leq 30^\circ$ . The notable dispersive dip feature from the

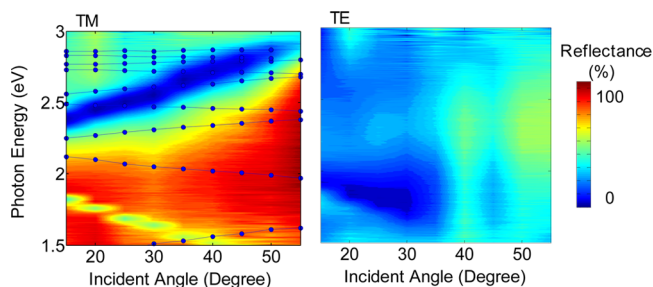


**Figure 2.** Angle-resolved reflectance spectra of the ZnO/Ag nanograting under illumination of (a) TM-mode and (b) TE-mode polarized light. Blue lines with filled circles in (a) represent the energy of the photon allowing grating-coupled SPP excitation at each incident angle (see Supporting Information Figure S2).

TM mode was similar to signature SPP excitation observed in previous studies.<sup>11–19</sup> Periodic metallic structures can allow multi-mode SPP excitation, whose energy is determined by the periodicity and dielectric functions of the constituent materials.

In a periodic structure, SPPs can be excited by incident photons, while the momentum mismatch is compensated according to the relationship  $k_{\text{SPP}} = k_{\text{ZnO}} \sin \beta \pm (2\pi/D)m$ , where  $k_{\text{SPP}}$  is a wave vector of the SPP at the ZnO/Ag interface,  $k_{\text{ZnO}}$  is a wave vector of the photon in the ZnO layer,  $\beta$  is the incident angle of the photon with respect to the surface normal of the Ag layer (Figure 1),  $D$  is the period of the grating, and  $m$  is an integer.<sup>11–18</sup> The symbol in Figure 2a represents the energy of the photon that allows grating-coupled SPP excitation at each incident angle (see supporting information Figure S2). Most of the symbols are located in the region with lower reflectance, assuring that part of the incoming photon energy is transferred to the SPPs propagating along the ZnO/Ag interface. Some deviations may be attributed to the detailed geometric parameters of the grating (width and height of the grooves)<sup>7</sup> and the finite thickness of the ZnO layer.<sup>18</sup>

Reflectance spectra and electric field distributions in the nanogratings were obtained by finite-difference time-domain (FDTD) simulations (Lumerical FDTD Solutions 7.0.1). Details of the calculations were similar to those used in our earlier study.<sup>11</sup> As shown in Figure 3, the calculated TM mode

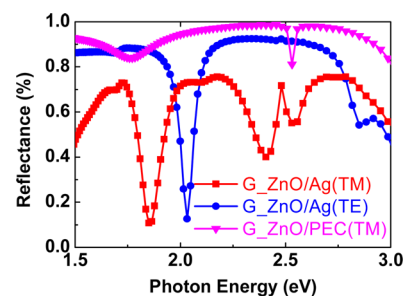


**Figure 3.** Simulated optical reflectance spectra of ZnO/metal nanogratings. Red and blue lines correspond to the TM and TE mode spectra of the ZnO/Ag nanograting, respectively. Magenta line indicates TM mode reflectance of a ZnO/PEC (perfect electric conductor) nanograting for comparison.

reflectance spectra of the ZnO/Ag grating showed three distinct dips (1.8, 2.4, and 2.5 eV), similar to the experimental results (Figure 2a). To clarify the origin, simulations were also performed for ZnO/PEC (perfect electric conductor) nanograting, which exhibited two dips at 1.75 and 2.55 eV in the TM mode. A PEC does not allow excitation of SPPs; thus, another mechanism must be responsible for the two dips. Metallic gratings can exhibit intriguing optical reflectance spectra. Intensive investigations have revealed that such anomalies originate from standing wave generation in the grooves, as well as the propagating SPPs.<sup>3–6,16–19</sup> This suggests that not only SPP excitation, but also the cavity mode, could contribute to the TM mode reflectance dips of the ZnO/Ag sample.

Figure 3 also shows the TE-mode reflectance spectra of the ZnO/Ag nanograting, which has a notable dip at 2.0 eV. Zuniga-Segundo and Mata-Mendez discussed field enhancement and reflectance dips of conducting grooves using modal theory.<sup>5</sup> Wirgin and Maradudin claimed significant field enhancement in a conducting lamellar grating; however, resonant dips in the far-field reflectance were not observed.<sup>6</sup> Metallic grooves were studied in these earlier works, but ZnO

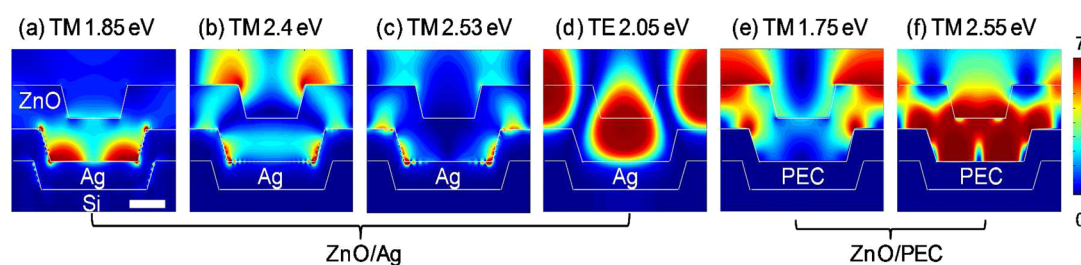


**Figure 4.** Electric field intensity distributions in the ZnO/Ag and ZnO/PEC nanogratings for several photon energies. The scale bar is 100 nm. (a–c) TM mode for ZnO/Ag, (d) TE mode for ZnO/Ag, and (e–f) TM mode ZnO/PEC.

thin films filled the grooves in our ZnO/Ag nanograting. Thus, the field enhancement in the grooves can induce strong absorption in the ZnO layer, resulting in reflectance dips. The TE mode reflectance near 2.0 eV was lower than that for other photon energies, as shown in Figure 2b. Such agreement between the calculation and experimental results indicates cavity resonance in the TE mode at 2 eV. The width and depth of the groove may be irregular in the fabricated sample, which can induce much broader features in the experimental spectra, compared with the simulation data.

Optical diffraction effects should also be considered for our ZnO/Ag nanogratings, to understand the reflectance spectra. Calculations showed that even the lowest-order diffraction is allowed only in the case for photon energies exceeding 2.75 eV, and  $\alpha \geq 60^\circ$  (see Supporting Information Figure S3). Therefore, the measured optical reflectance spectra in Figure 2a and b were not much affected by diffraction. The regime influenced by diffraction was very limited, due to the relatively short grating period and the large refractive index of ZnO in the visible range.

Figure 4a–f shows electric field intensity distributions in the ZnO/Ag gratings at photon energies corresponding to the reflectance dips of the simulation data (Figure 3). In Figure 4a–c, significant field confinement at the ZnO/Ag interface appears, indicating SPP excitation. A strong electric field confined in the groove filled with the ZnO layer is also observed, in particular in Figure 4a. Such strong field formation, caused by cavity resonance, can enhance the absorption in the ZnO layer, resulting in the reflectance dips, as discussed above. This suggests that these TM mode reflectance dips  $>2.0$  eV were produced by hybrid-mode (cavity resonance and SPP) formation.<sup>9</sup> In the TE mode, notable field enhancement in the ZnO layer is observed at 2.05 eV (Figure 4d). This clearly shows that the cavity resonance was the origin of the 2.0 eV dip in the TE mode reflectance spectra (Figure 3). When the Ag layer in the nanograting was replaced with a PEC layer, strong field in the ZnO layer is observed at photon energies of 1.75 and 2.55 eV (Figure 4e and f). Such field enhancement is originated from the cavity resonance without doubt. Therefore, similarity in the field distribution in the ZnO/Ag (Figure 4a–c) and ZnO/PEC (Figure 4e–f) structures assures the cavity resonance in the ZnO/Ag nanogratings.

Figure 5 shows the micro-PL spectra of the ZnO/Ag nanograting and a planar ZnO/Ag thin film: both of the nanograting and the planar samples have identical thickness of the ZnO (120 nm) and Ag (80 nm) layers. The PL spectra of the planar sample consist of a peak at  $\sim 3.2$  eV, originating from the near-band-edge transitions, and a broad peak in the visible range due to defect electronic states inside the bandgap region. The overall PL intensity of the nanogratings increases

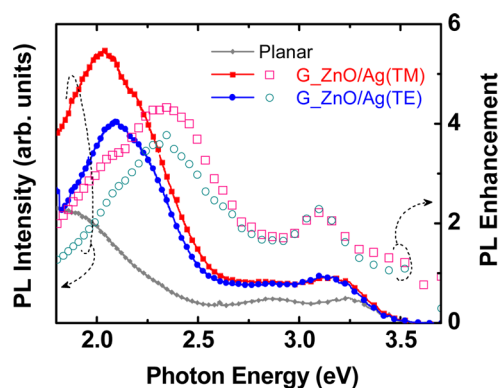


**Figure 5.** PL spectra of the ZnO/Ag nanograting (lines with filled symbols – red for TM mode and blue for TE mode) and a planar ZnO/Ag thin film (line with “gray” filled symbols). The thickness of the ZnO and Ag layers are identical in both of the nanograting and the planar sample. PL enhancement indicates the ratio of the PL intensity of the nanograting to that of the planar thin film (open symbols – red for TM mode and blue for TE mode).

significantly for both the TM and TE modes, compared with that of the planar counterpart. The grating-coupled SPPs propagate along the ZnO/Ag interface. Photons radiated from the SPPs, as well as from the directly incident light, can generate electron–hole pairs in the ZnO layer. Subsequent recombination results in light emission from the nanograting. Such a scenario can well explain the TM-mode PL enhancement, as reported by our research group earlier.<sup>11</sup> Strong-field build-up in the ZnO layer was also observed in the TE mode, which can be attributed to cavity resonance (Figure 4d). Consequently, the large electric field intensity helps increase of the PL intensity. Thus, both the cavity resonance and SPP excitation can raise the PL intensity in the TM mode. In the TE mode, cavity resonance enhances the PL intensity. Such enhancement can raise the visible-range light emission, because the energies are less than 3 eV, as discussed above. Thus, the band-to-band emission is enhanced, mainly due to the volume increase in the ZnO layer in the grating structure. We should note that the SPP-mediated enhancement is possible only in the TM mode using a 1D grating.<sup>14–18</sup> In our ZnO/Ag nanograting, combination of the SPP effects and cavity resonance enables enhanced light emission. It should be noted that the semiconductor/metal grating structures show angle-dependent PL spectra determined by the dispersion relations of SPP and guided modes.<sup>16,17</sup> Therefore, such directional and enhanced emission properties can be optimized for specific intended applications.

## CONCLUSION

ZnO/Ag nanograting structures, fabricated by e-beam lithography and dry etching, exhibited much enhanced PL intensity under both TM- and TE-mode light: 400% larger than that of the planar sample. In contrast, the angle-resolved optical reflectance spectra showed distinct behaviors that depended on the incident light polarization. In the TM mode, dispersive dips were clearly observed. The field distribution maps, obtained by FDTD simulations, confirmed SPP excitation and the cavity mode inside the grating groove at corresponding reflectance dips. In the TE mode, a very broad dip with little angle dependence was observed. The simulation showed that such a dip should have originated from cavity resonance. The cavity resonance, as well as SPP excitation, enhanced the electric field intensity in the ZnO layer, enabling polarization-insensitive PL intensity enhancement.

## ASSOCIATED CONTENT

### Supporting Information

SEM image, SPP dispersion relation, and diffraction calculation. This material is available free of charge via the Internet at <http://pubs.acs.org>.

## AUTHOR INFORMATION

### Corresponding Author

\*Phone: +82 2 3277 6668. Fax: +82 2 3277 2372. E-mail: [dwkim@ewha.ac.kr](mailto:dwkim@ewha.ac.kr).

### Notes

The authors declare no competing financial interest.

## ACKNOWLEDGMENTS

This work was supported by the Pioneer Research Center Program (2009-0083007) and the Quantum Metamaterials Research Center (2008-0061893) through the National Research Foundation of Korea Grant. This work was also supported by the New & Renewable Energy Technology Development Program of the Korea Institute of Energy Technology Evaluation and Planning (KETEP) Grant (20123010010160).

## REFERENCES

- (1) Wood, R. W. On a Remarkable Case of Uneven Distribution of Light in a Diffraction Grating Spectrum. *Proc. R. Soc. London, Ser. A* **1902**, *18*, 269.
- (2) Fano, U. The Theory of Anomalous Diffraction Gratings and of Quasi-stationary Waves on Metallic Surfaces. *J. Opt. Soc. Am.* **1941**, *31*, 213.
- (3) Hessel, A.; Oliner, A. A. A New Theory of Wood's Anomalies on Optical Gratings. *Appl. Opt.* **1965**, *4*, 1275–1297.
- (4) Ritchie, R. H.; Arakawa, E. T.; Cowan, J. J.; Hamm, R. N. Surface-Plasmon Resonance Effect in Grating Diffraction. *Phys. Rev. Lett.* **1968**, *21*, 1530–1533.
- (5) Zuniga-Segundo, A.; Mata-Mendez, O. Interaction of S-polarized Beams with Infinitely Conducting Grooves: Enhanced Fields and Dips in the Reflectivity. *Phys. Rev. B* **1992**, *46*, 536–539.
- (6) Wirgin, A.; Maradudin, A. A. Resonant Enhancement of the Electric Field in the Grooves of Bare Metallic Gratings Exposed to S-polarized Light. *Phys. Rev. B* **1985**, *31*, 5573–5576.
- (7) Lopez-Rois, T.; Mendoza, D.; Garcia-Vidal, F. J.; Sanchez-Dehesa, J.; Pannetier, B. Surface Shape Resonances in Lamellar Metallic Gratings. *Phys. Rev. Lett.* **1998**, *81*, 665.
- (8) Ebbesen, T.W.; Lesec, H. J.; Ghaemi, H. F.; Thio, T.; Wolff, P. A. Extraordinary Optical Transmission Through Sub-wavelength Hole Arrays. *Nature (London)* **1998**, *391*, 667.

(9) Garcia-Vidal, F. J.; Martin-Moreno, L. Transmission and Focusing of Light in One-Dimensional Periodically Nanostructured Metals. *Phys. Rev. B* **2002**, *66*, 155412.

(10) Dufaux, T.; Dorfmueller, J.; Vogelgesang, R.; Burghard, M.; Kern, K. Surface Plasmon Coupling to Nanoscale Schottky-type Electrical Detectors. *Appl. Phys. Lett.* **2010**, *97*, 161110.

(11) Gwon, M.; Lee, E.; Kim, D.-W.; Yee, K.-J.; Lee, M. J.; Kim, Y. S. Surface-Plasmon-Enhanced Visible-Light Emission of ZnO/Ag Grating Structures. *Opt. Express* **2011**, *19*, 5895–5901.

(12) Lawrie, B. J.; Kim, K.-W.; Norton, D. P.; Haglund, R. F. Plasmon–Exciton Hybridization in ZnO Quantum-Well Al Nanodisc Heterostructures. *Nano Lett.* **2012**, *12*, 6152–6157.

(13) Chen, H.-Y.; Liu, K.-W.; Jiang, M.-M.; Zhang, Z.-Z.; Liu, L.; Li, B.-H.; Xie, X.-H.; Wang, F.; Zhao, D.-X.; Shan, C.-X.; Shen, D.-Z. Tunable Hybridized Quadrupole Plasmons and Their Coupling with Excitons in ZnMgO/Ag System. *J. Phys. Chem. C* **2014**, *118*, 679–684.

(14) Cui, X.; Tawa, K.; Kintaka, K.; Nishii, J. Tailored Plasmonic Gratings for Enhanced Fluorescence Detection and Microscopic Imaging. *Adv. Funct. Mater.* **2010**, *20*, 945–950.

(15) Tawa, K.; Umetsu, M.; Nakazawa, H.; Hattori, T.; Kumagai, I. Application of 300× Enhanced Fluorescence on a Plasmonic Chip Modified with a Bispecific Antibody to a Sensitive Immunosensor. *ACS Appl. Mater. Interfaces* **2013**, *5*, 8628–8632.

(16) Frisecheisen, J.; Niu, Q.; Abdellah, A.; Kinzel, J. B.; Gehlhaar, R.; Scarpa, R.; Adachi, C.; Lugli, P.; Brütting, W. Light Extraction from Surface Plasmons and Waveguide Modes in an Organic Light-Emitting Layer by Nanoimprinted Gratings. *Opt. Express* **2010**, *A7*, 2010.

(17) Wang, C.-M.; Tsai, Y.-L.; Tu, S.-H.; Lee, C.-C.; Kuo, C.-H.; Chang, J.-Y. Optical Properties of Light Emitting Diodes with a Cascading Plasmonic Grating. *Opt. Express* **2010**, *18*, 25608.

(18) Haug, F.-J.; Söderström, T.; Cubero, O.; Terrazoni-Daudrix, V.; Ballif, C. Plasmonic Absorption in Textured Silver Back Reflectors of Thin Film Solar Cells. *J. Appl. Phys.* **2008**, *104*, 064509.

(19) Ferry, V. E.; Verschuuren, M. A.; van Lare, M. C.; Schropp, R. I. E.; Atwater, H. A.; Polman, A. Optimized Spatial Correlations for Broadband Light Trapping Nanopatterns in High Efficiency Ultrathin Film a-Si: H Solar Cells. *Nano Lett.* **2011**, *11*, 4239–4245.